Tidal rhythmites and their implications

Rajat Mazumder[*], Makoto Arima

*Geological Institute, Graduate School of Environment and Information Sciences, Yokohama National University,
79-7, Tokiwadai, Hodogaya, Yokohama 240 8501, Japan*

Received 22 March 2004; accepted 7 July 2004

Abstract

Tidal rhythmites are unequivocal evidence of marine conditions in sedimentary basins and can preserve a record of astronomically induced tidal periods. Unlike modern tide and tidal deposits, analysis of ancient tidal rhythmites, however, is not straightforward. This paper highlights the advances made in the tidal rhythmite research in the last decade and reviews the methodologies of extracting lunar orbital periods from ancient tidal rhythmites, the mathematics behind the use of tidalites, and their limitations and uncertainties. We have shown that analysis of ancient tidal rhythmite may help us to estimate the palaeolunar orbital periods in terms of lunar days/month accurately. Determination of absolute Earth–Moon distances and Earth's palaeorotational parameters in the distant geological past from tidal rhythmite, however, is ambiguous because of the difficulties in determining the absolute length of the ancient lunar sidereal month.
© 2004 Elsevier B.V. All rights reserved.

Keywords: Tidal rhythmites; Lunar orbital period; Earth–Moon distance; Palaeogeophysics; Universal gravitational constant

1. Introduction

Tidal rhythmites are packages of laterally and/or vertically accreted, laminated to thinly bedded medium- to fine-grained sandstone, siltstone and mudstone of tidal origin that exhibit rhythmic change in lamina/bed thickness and grain-size (Williams, 1991; Kvale, 2003). In the absence of fossils, these physical sedimentary structures provide unequivocal evidence of marine conditions in sedimentary basins (cf. Eriksson et al., 1998; Eriksson and Simpson, 2004). Tidal rhythmites have been used to interpret palaeoclimate (Kvale et al., 1994; Miller and Eriksson, 1997) and palaeo-ocean seiches (Archer, 1996a). Tidal rhythmites can preserve a record of astronomically induced tidal periods, and are the only unambiguous tool available for tracing the evolutionary history of the Earth–Moon system (Williams, 1989, 2004; Sonett et al., 1996; Kvale et al., 1999). Multidisciplinary research in the last decade has demonstrated that the palaeolunar orbital dynamics can be determined through integrated analyses of ancient tidal rhythmites in combination with an understanding of basic tidal

theory (cf. Sonett et al., 1988, 1996; de Boer et al., 1989; Piper, 1990; Archer et al., 1991; Archer, 1996b; Oost et al., 1993; Rosenberg, 1997; Kvale et al., 1999; Williams, 2000, 2004).

Unlike modern tide and tidal deposits, analysis of ancient tidal rhythmites, however, is not straightforward. The accuracy of palaeotidal periods depends upon a number of factors and palaeorotational parameters (Earth–Moon system parameters) must be geophysically valid to directly trace the early history of Earth's tidal deceleration and the evolving lunar orbit with confidence (Williams, 1997, 2000, 2004). As Williams (2000) pointed out, detailed analyses of ancient tidal rhythmites would greatly enrich our knowledge of the dynamical history of the Earth–Moon system. This paper highlights the nature of advancements made in the tidal rhythmite research methodology in the last decade. It discusses the astronomical control on rhythmite generation, explains methodologies for extracting lunar orbital periods from the ancient tidal rhythmite record, and review the use of tidalites, the mathematics behind their use, and their limitations and uncertainities.

2. Control on tidal rhythmite generation

2.1. Astronomical forcing

To gain insight into the palaeoastronomic significance of ancient tidal rhythmites, it is essential first to understand the astronomical control on tide and tidal rhythmite generation. The equilibrium tidal theory considers tractive gravitational forces of the Moon and Sun on an idealized Earth completely covered by deep water of uniform depth that is capable of instantly responding to changes in tractive forces (Macmillan, 1966; Kvale et al., 1999). Although the equilibrium tidal theory is helpful in understanding the basic tidal cycles that influence tidal sedimentation systems, it is of little use in analyzing the tidal rhythmites. This is because the real oceanic tides do not conform to equilibrium tidal theory (cf. Pugh, 1987).

2.1.1. The Earth–Moon–Sun rotational system

Oceanic tides are the periodic rise and fall of the sea level as a direct consequence of the combined gravitational attraction of the Moon and Sun on the Earth. Three basic astronomical movements control the tidal pulses within the Earth–Moon–Sun rotational system. These are: (1) the Earth's rotation about its own axis with a period of 1 day; (2) the Moon's revolution around the Earth in an elliptical orbit with a periodicity of 29 days; and (3) the Earth's revolution around the Sun in an elliptical orbit with a period of 365.25 days (Russell and MacMillan, 1970). It is important to note that all the periods were likely of different duration in the geological past. The observed tidal pattern occurring at a particular point on the Earth's surface is the sum of a number of harmonic components associated with lunar and solar astronomical cycles (Brown et al., 1989; Martino and Sanderson, 1993).

Interaction of gravitational forces of the Moon and Sun on the Earth results in two centers of tidal heaping at the point on the Earth's surface closest to, and farthest away from, the Moon (Fig. 1; de Boer et al., 1989). A point on the Earth's surface passes twice through areas of tidal heaping in 24 h as a result of the Earth's rotation on its axis. This gives rise to the semidiurnal periodicity (2 tides/day) of the Earth's tide similar to the tides of the Atlantic coast of the United States. In purely diurnal tidal systems similar to those of the northern shore of the Gulf of Mexico and the Java Sea, the semidiurnal tidal components are suppressed and the duration of the flood–ebb cycle is around 24 h (i.e. 1 tide/day). All intermediate tidal systems are classified as mixed tidal systems (1–2
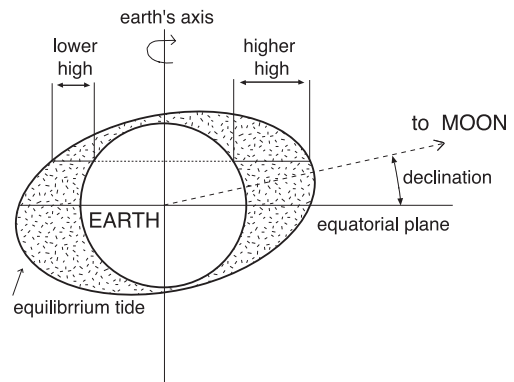

Fig. 1. A schematic representation of the tidal effect of the Moon on Earth. The tidal forces result maximum elevations of water level at the points closest to and farthest away from the Moon on Earth (modified after de Boer et al., 1989).

tides/day) depending on the relative importance of the diurnal and semidiurnal components (Russell and MacMillan, 1970). Most ($\approx 90\%$) of the modern tidal systems are mixed or semidiurnal in nature. Purely diurnal tidal system accounts for only 10% of the observations (Lisitzin, 1974).

2.1.2. Variability in the Moon's gravitational pull

2.1.2.1. Monthly variation. In addition to the daily patterns, tidal systems are also influenced by the variability in the gravitational pull on the Earth due to (1) the changing phases of the Moon, (2) declination of the Moon and (3) the changing Earth–Moon distance during the lunar orbit. The Moon's gravitational pull on the Earth is maximum (spring) when the Earth, Moon and Sun are aligned (syzygy, full or new) and minimum (neap) when the radius vector to the Sun and the Moon from the Earth form a right angle (quadrature). The neap–spring (half-synodic, syzygy to syzygy) tidal period is thus related to the changing phases of the Moon. The synodic month (new Moon to new Moon) has a modern period of 29.53 days.

The lunar orbital plane is inclined to the Earth's equator at an angle of $23°27'$. The movement of the Moon between its extreme declinations across the Earth's equator induces diurnal inequality of the tide in the semidiurnal tidal systems (de Boer et al., 1989; Kvale et al., 1999). The diurnal inequality is greatest when the Moon is at its maximum declination and is reduced to zero when the Moon is over the equator. The equatorial passage of the Moon is known as crossover that gives rise to two subsequent semidaily tides of equal strength (Kvale et al., 1999, their Fig. 3). The time it takes the Moon to orbit the Earth moving from its maximum northern declination to its southern declination and the return, a tropical month, has a modern period of 27.32 days.

The distance between the Earth and Moon changes by about 11% during a lunar month, resulting in a 35% variation in the tidal height (cf. Stowe, 1987; Martino and Sanderson, 1993). This is because the Moon's orbital travel along the elliptical path carries it between perigee and apogee, closest and farthest distance from the Earth, respectively. The time it takes the Moon to move from perigee to perigee, an anomalistic month, has a modern period is 27.55 days.

2.1.2.2. Multiyear variation. Some multiyear astronomically controlled cycles affect the tidal depositional systems. These include the lunar nodal (modern period 18.6 years) and apsides cycle (modern period 8.85 years). The lunar nodal cycle is a consequence of the nutation of the lunar orbital plane that changes the declination of the lunar orbital plane relative to the Earth's equator from $18°$ to $28°$ and back every 18.6 years. The lunar nodal cycle exerts control on the tidal amplitude (cf. Kaye and Stuckey, 1973). For example, the tidal amplitude near Delfzijl (NE Netherlands) varies from 2.8% to 5.2% with the variation of the lunar orbit (Oost et al., 1993, their Fig. 2). The tidal current strength is proportional to tidal amplitude. It has been shown that a 5.2% increase in tidal amplitude would result in a 15–20% increase in sediment transport capacity (cf. Oost et al., 1993, p. 3). Wells and Coleman (1981) considered the periodic migration of mudflats along the Guiana Coast have been caused by the successful colonization of the mudflats by *Avenicennia mangrove* propagules. The successful colonization was possible because of lower mean sea level and hence, prolonged exposure during periods of tidal minima caused by the 18.6 years and solar semiannual tidal components (Wells and Coleman, 1981; see also Oost et al., 1993). Allen (1990) recognized the variation of maximum tidal heights due to the influence of lunar nodal cycle and considered it in a computational model for salt-marsh growth. Oost et al. (1993) have shown that the 18.6-year nodal cycle modulates tidal amplitudes and currents, and consequently sedimentation in tide-influenced modern sedimentary environments. These authors have suggested that sedimentary processes in tide-influenced sedimentary environments are rarely that regular that continuous sequences, reflecting the nodal cycle, will be preserved. However, if preserved, tide-influenced deposits bearing the imprint of the lunar nodal cycle may be found in accretionary deposits of continuously migrating inlets, the fill of abandoned channels, the growth of regressive barrier beach islands and the vertical accretion of supra-tidal marsh deposits (Oost et al., 1993, p. 10). Tides raised on the Earth by the Moon and Sun show a 8.85-year periodicity, known as lunar apsides period, related to the orbital advance of the Moon at perigee. Unlike the lunar nodal cycle, the lunar apsides cycle, however, exerts much less control on the tidal amplitude

(Fairbridge and Sanders, 1987; Marchuk and Kagan, 1989; Oost et al., 1993). Ancient sediments rarely record the imprint of lunar nodal cycles, because nearly two decades of uninterrupted sedimentation must be preserved (cf. Oost et al., 1993; Miller and Eriksson, 1997). Walker and Zahnle (1986) interpreted a 23.3±0.3-year periodicity preserved in 2500 Ma old Weeli Wolli banded iron formation as reflecting the climatic influence of lunar nodal cycle. Williams (1989) reported both the lunar nodal (19.5 years) and apsides (9 years) cycles from the Neoproterozoic (620 Ma) Elatina tidal rhythmite, Australia. Miller and Eriksson (1997) recognized a multiyear cyclicity from Late Mississippian Pride shale, Virginia where 17–22 annual beds display a crude upward thickening and thinning within meter-scale bundles. This bundling is interpreted to reflect the 18.6-year nodal cycle with the thick annual beds representing years during which the inclination of the lunar orbital plane favored increased tidal amplitudes (Miller and Eriksson, 1997).

2.2. Non-tidal influence

In addition to the astronomical forcing, influences of meteorological storms, atmospheric pressure, salinity, water temperature, precipitation and climatically or seasonally controlled sea level change may be superimposed on the tidal cycles, which, in turn, control tidal rhythmite generation. These non-tidal influences on the tidal rhythmite generation are often responsible for the deviation from the predicted monthly tidal periodicities (Yang and Nio, 1985; de Boer et al., 1989; Kvale et al., 1999; discussed below). Additionally, bioturbation can destroy or obscure the tidal record.

3. Research methodology

3.1. Bed/lamina thickness measurement

Tidal signatures in the ancient sedimentary successions are preserved either as vertically accreted flat-laminated rhythmite (e.g. the Elatina-Reynella, Big Cottonwood, and the Jackson Lake rhythmite, Williams, 1989, 2000; Chan et al., 1994; Mueller et al., 2002) or as laterally accreted bundles of sandstone

foresets separated by mudstone drapes (Fig. 2; cf. de Boer et al., 1989; Deynoux et al., 1993; Bose et al., 1997; Eriksson and Simpson, 2000a, 2004; Mueller et al., 2002; Tape et al., 2003; Mazumder, 2004). The effectiveness of the tide as an agent of sediment transport and deposition is directly related to tidal range and consequent current velocity (FritzGerald and Nummedal, 1983; Boothryod, 1985; Williams, 2000). Large tidal ranges result in relatively thick deposits whereas smaller tidal ranges result in thinner deposits. In semidiurnal tidal systems, as many as four lamina may be deposited in 24 h. Within a neap–spring–neap cycle of a modern semidiurnal tidal system, an average of 28 dominant current events (lamina) can be recorded. In pure diurnal systems, however, only 14 dominant current events occur in a neap–spring–neap cycle. In a modern mixed tidal system, the number of dominant current events is between 28 and 14 within a neap–spring cycle. Thus, plotting of successive thickness in a lamina number vs. thickness plot provides us valuable information regarding the nature of the palaeotidal system (cf. de Boer et al., 1989; see Section 3.3 for explanation).

Ancient tidal rhythmite records are commonly incomplete. Incomplete data sets may result in several ways. A tidal depositional system may filter out the effects of the lesser semidiurnal components of diurnal inequality (de Boer et al., 1989; Williams, 2000) when it is too weak to transport sediment to the depositional

Fig. 2. Laterally accreted tidal rhythmite from the Protoproterozoic Chaibasa sandstone, India. Note double mud drape and characteristic thick–thin alternations in foreset laminae thickness. These features suggest that the Chaibasa sandstones were deposited in a subtidal setting (pen length 14 cm; after Bose et al., 1997).

site. The tidal range and current speed are minimum at position of neap tides. As a consequence, the deposition of sandy and silty laminae may be interrupted in the distal offshore depositional settings. Incompleteness in tidal rhythmite data may be also due to the periodically low sediment yields during summer or bioturbation. In shallow marine depositional settings, meteorological storms often interrupt normal tidal sedimentation patterns. As a result, the number of bed/laminae is lesser than what is expected in an ideal situation. This incomplete data set is the major impediment to recover lunar orbital periodicities from simple counting of lamina. Completeness of the annual tidal cycle can be evaluated by checking whether every neap–spring cycle is represented in the annual cycle. There are two spring tides in a lunar month. However, these spring tides are of unequal magnitude, producing high- and low-spring tides that correspond to spring tides during or near perigee (high spring) and spring tides during or near apogee (low spring), respectively. The semimonthly inequality of the spring tides is called phase flip (cf. Kvale et al., 1999, their Fig. 5B). Ideally, a complete tidal rhythmite data set should show a continuous thick–thin alternation, with phase flip about once during each neap–spring cycle. Deviations from the thick–thin–thick pattern of course may occur, e.g. due meteorological events, but when that is the case, the same rhythm should be resumed afterwards. If the data set is incomplete, then a careful look may reveal 180° phase change of the thick–thin pattern indicating that the data set contains at least some hiatus (Poppe L. de Boer, personal communication, 2003; see also Kvale et al., 1999).

3.2. Harmonic analysis

It is possible to unlock the lunar orbital periods through harmonic analysis of long tidal rhythmite data provided the data set is complete (cf. Williams, 1989, 2000; Archer, 1996a; Archer et al., 1991; Kvale et al., 1995, 1999). Harmonic analysis resolves a sinusoidal function (time sequence) into sinusoidal (harmonic) components with commensurate frequencies, the contributions from each component being indicated by its amplitude or power (the square of amplitude) (Jenkins and Watts, 1968; Yang and Nio, 1985). The output (power spectrum) is displayed by plotting the power of the harmonic components against its

frequency. In the tidal context, harmonic analysis makes use of the knowledge that the observed tide is the sum of a number of components, whose periods precisely corresponds with the period of one of the relative astronomical motions in the Earth–Moon–Sun rotational system. A record of tidal height (or tidal current velocity) over a long time-span is required to determine the amplitude and frequency for each harmonic component in the modern tidal depositional settings. As mentioned earlier, the amount of sediment transported and ultimately deposited as a tidal rhythmite is related to tidal height (i.e. tidal range). Therefore, it is the successive lamina/bed thickness data that is used while recovering palaeolunar orbital periods by harmonic analysis. Fast Fourier trans-
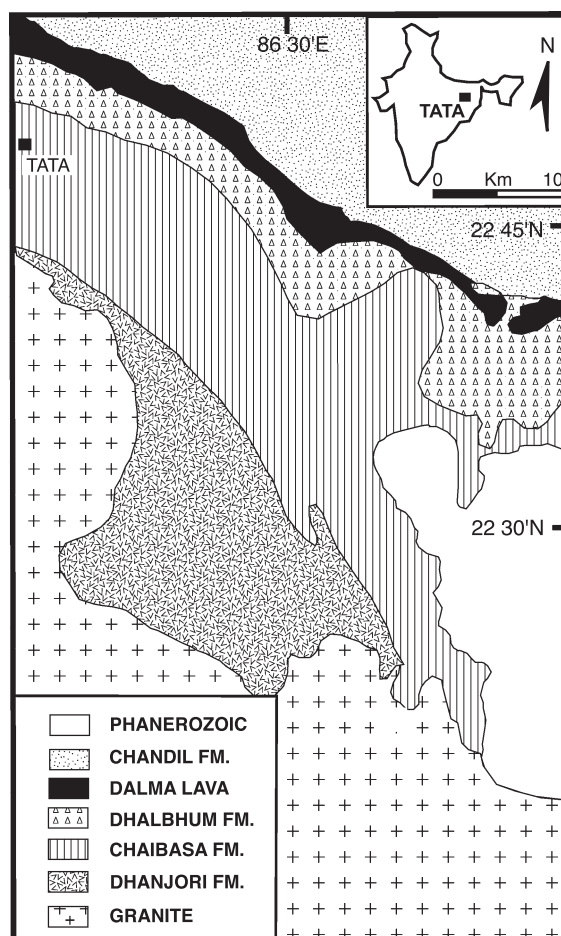

Fig. 3. Simplified geological map showing the Chaibasa and its bounding formations, eastern India (modified after Saha, 1994).

formations (FFT) and maximum entropy methods (MEM) are particularly useful for separating overlapping periodicities (cf. Press et al., 1989; Archer et al., 1991; discussed below).

3.3. Late Paleoproterozoic Chaibasa tidal rhythmite (India)—a case study

The 6- to 8-km-thick, entirely siliciclastic late Paleoproterozoic Chaibasa Formation (Fig. 3) constitutes the lower part of the two-tiered Singhbhum Group, comprising rocks metamorphosed to greenschist (locally amphibolite) facies (Naha, 1965; Saha, 1994; Mazumder, 2002). Lithologically, it is characterized by the interbedding of sandstones and shales in different scales. Although the Chaibasa sandstones formed in a subtidal setting, the shales formed in a distal offshore setting and represent marine flooding surfaces (Bose et al., 1997; Mazumder, 2002). The Chaibasa succession is generally transgressive with intermittent punctuations caused by short-term lowstands during which sandstones were emplaced
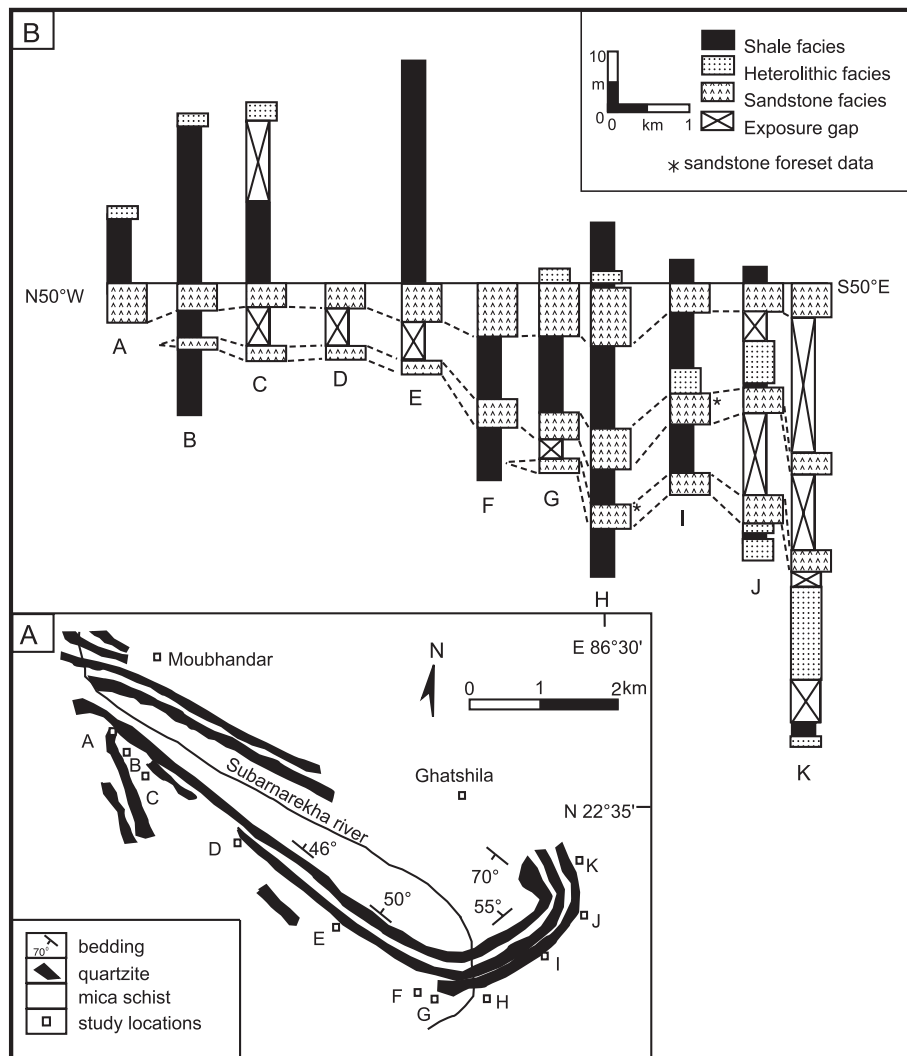

Fig. 4. (A) Geological map showing lithounits (Chaibasa Formation) in and around Ghatshila (modified after Naha, 1965). (B) Panel diagram showing lateral and vertical facies transition during Chaibasa sedimentation; study locations are marked in A (modified after Bose et al., 1997).

(Mazumder et al., 2000; Mazumder, 2002; cf. Cattaneo and Steel, 2003).

The cross-bedded Chaibasa sandstone (Figs. 2 and 4A,B) is best exposed in and around Ghatshila (Fig. 4A). The sandstones are generally well sorted and internally characterized by unidirectional cross-strata (set thickness up to 65 cm). The thick–thin laminae alternations are characteristic as is a double mud drape (Fig. 2). The cross-bed set is characterized by sandstone foresets separated by mudstone drapes (Fig. 2). The abundance and thickness of mudstone drapes vary across the set; they show an inverse relationship to the foreset thickness in the sandstone: drapes are thinner and relatively rare in intervals of thick foresets and abundant and thicker in intervals of thin foresets (cf. Tape et al., 2003). Laminae thickness is measured perpendicular to the dip of the foresets along a horizontal line between the upper and lower bounding surfaces. Cyclicities are revealed in plots of two successive foreset-thickness data sets (Figs. 5A and 6A) measured from different stratigraphic levels from exposures southeast of Ghatshila (Fig. 4A,B). Random meteorological events like storms may impart thick–thin alternations in environments that lack semidiurnal tidal influence. Alternatively, semidiurnal thick–thin laminae alternations may be disturbed by such meteorological events (cf. de Boer et al., 1989). A statistical test of the basic data has therefore been made, following the methodology of de Boer et al. (1989), which reveals a significant semidiurnal signal (Figs. 5A and 6A). The number of foreset laminae, constituting neap–spring cycles, varies from 27 to 30.

Harmonic analysis following the methodology of Archer et al. (1991) and using a fast Fourier transform (FFT) program (Horne and Baliunas, 1986; Press et al., 1989) was performed on both data sets. The program tests for cyclicities and is capable of separating cycles having closely spaced periodicities. The output is expressed as an event/cycle in a frequency vs. power spectral-density plot (Figs. 5B and 6B).

Power spectral-density plots show spectral periods of 32 events that represent neap–spring cycles, analogous to those derived from the analysis of modern tides as well as from the ancient record (Figs. 5B and 6B) (Archer et al., 1991; Kvale et al., 1995; Williams, 2000). Both the power spectra exhibit a spectral period of ~2. This result, coupled with the occurrence of alternating, millimeter-scale, thick–thin
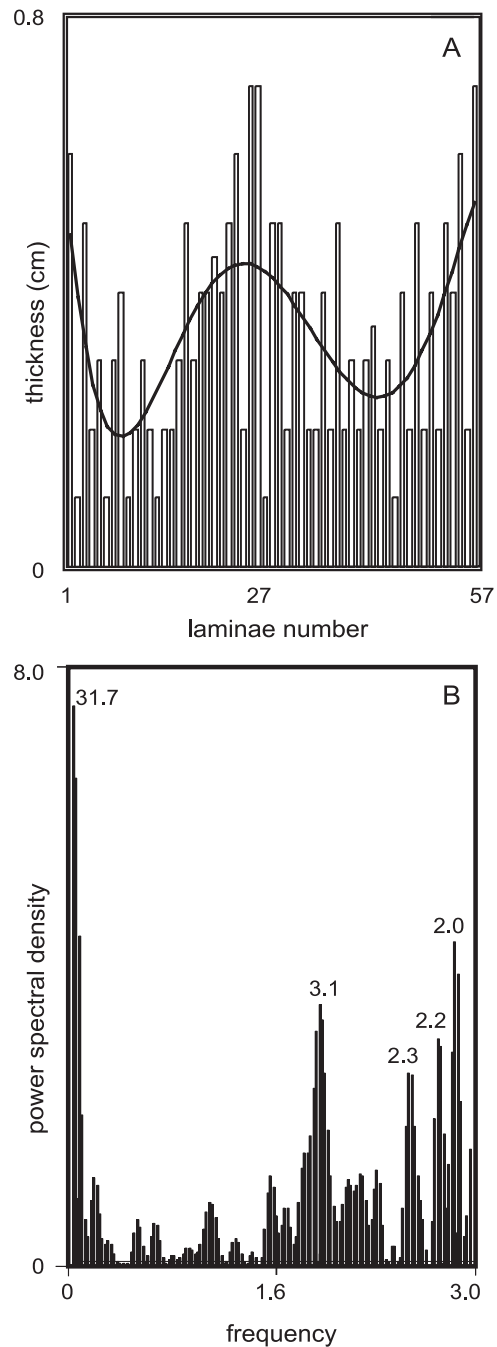

Fig. 5. Analysis of the cross-stratified sandstone (data collected from the second quartzite band from the bottom, see Fig. 4B). (A) Thickness variations in successive foresets (*n*=57). (B) FFT power spectral plot (unsmoothed) obtained from the data set presented in A. Note the spectral periods around 32 and 2.
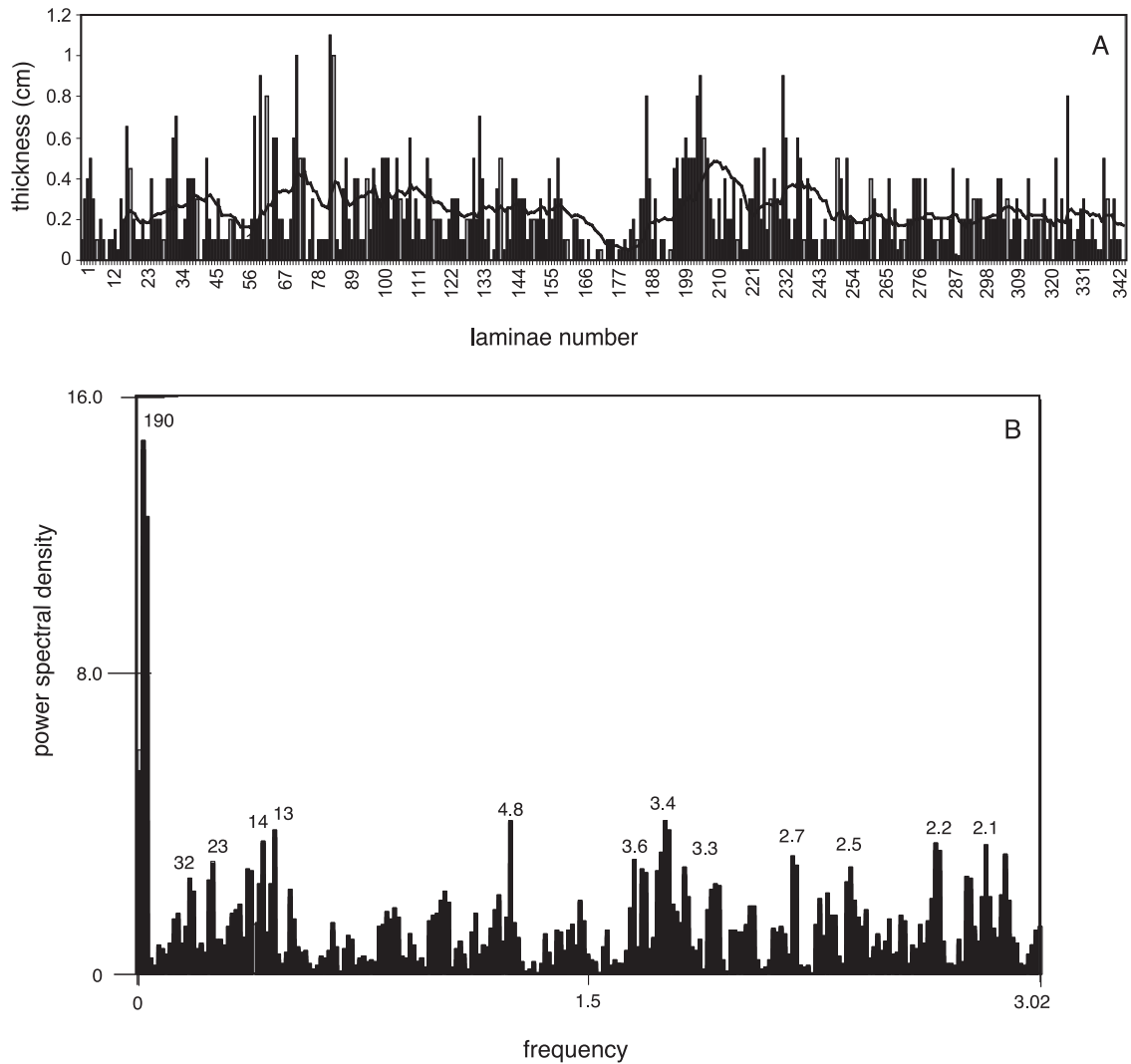
Fig. 6. Analysis of the cross-stratified sandstone (data collected from the first quartzite band from the bottom, see Fig. 4B). (A) Thickness variations in successive foresets (n=345). (B) FFT power spectral plot (unsmoothed) obtained from the data set presented in A. Note the spectral periods around 32 and 2.

laminae (Fig. 2), corroborates a dominantly semi-diurnal tide during the Chaibasa sedimentation (cf. de Boer et al., 1989). Spectral peaks between 3–5 (Figs. 5B and 6B) and ~13 were likely generated by some random variations (storms?). The spectral peak at 23 might represent an abbreviated anomalistic period (cf. Archer, 1996a; Kvale et al., 1999). The spectral period of 190 events possibly indicates some long-period tidal (abbreviated half yearly cycle?) and/or non-tidal variation (cf. Yang and Nio, 1985).

In a dominantly semidiurnal tidal system, synodic (spring–neap–spring) periodicity dominates tropical periodicity (Kvale et al., 1999). As mentioned earlier, the laminae count reveals 27–30 laminae (events) constituting the neap–spring cycle during Chaibasa sedimentation. It is, however, difficult to recover the lunar orbital periods from the direct counting of lamina because periodically weak tidal currents (such as during neap tide) and random meteorological events (such as storms) may modulate or abbreviate

tidal periods (de Boer et al., 1989; Kvale et al., 1999). However, both the power spectra show a consistent spectral period at 32 (Figs. 5B and 6B). Thus, there are ~32 laminae in a neap–spring cycle, implying at least 32 lunar days per synodic month during the Chaibasa sedimentation. It is interesting to note that Williams (2000) counted as many as 28–30 laminae couplets per neap–spring cycle on enlarged photographs of thin sections of little-compacted chert nodules (his Fig. 14a) up to six to eight neap–spring cycles from the 2450 Ma Weeli Wolli banded-iron formation, Australia. He considered only those cycles those are devoid of any sort of abbreviation (Williams, 2000, p. 54). Williams (2000, his Table 1) calculated 31.1 ± 1.5 lunar days per synodic month during the early Paleoproterozoic. The minimum number of lunar days in a synodic month (32, Figs. 5B and 6B) and hence the minimum number of solar days per synodic month (~33 because the solar day is shorter than the lunar day; cf. Williams (2000) during the Chaibasa sedimentation agrees well with that calculated by Williams (2000), his Table 1, column 3).

4. Ancient tidal rhythmite research in the last decade

Ancient tidal rhythmite research in the last decade has highlighted their characteristics and unlocked the encoded tidal and/or non-tidal periodicities through harmonic analysis based on the information available from modern tidal settings (cf. Kvale et al., 1995). The modern analogues provide the actualistic basis for ancient rhythmite research (cf. Zaitlin, 1987; Dalrymple and Makino, 1989; de Boer et al., 1989; Dalrymple et al., 1991; Kvale et al., 1995; Archer and Johnson, 1997). Effort has been made to quantify tidal record from rhythmites as old as 3.2 Ga (Eriksson and Simpson, 2000a,b, 2001, 2004; Mazumder, 2001). Other well-documented Precambrian tidal rhythmites are from the Late Archaean of Canada (Mueller et al., 2002), Palaeoproterozoic of Australia (Williams, 2000) and India (Bose et al., 1997), from the Neoproterozoic of North America (Trisgaard, 1993; Chan et al., 1994; Archer, 1996a; Archer and Johnson, 1997) and Australia (Williams, 1989, 1991). Well-documented Paleozoic tidal rhythmites are from the upper Cambrian of southwest Minnesota (Tape et al., 2003), Permian of India (Ghosh et al., 2004), and from the Carboniferous of USA (Kvale et al., 1989; Kuecher et al., 1990; Brown et al., 1990; Archer and Kvale, 1993; Martino and Sanderson, 1993; Archer et al., 1994, 1995; Greb and Archer, 1995; Tessier et al., 1995; Miller and Eriksson, 1997; Adkins and Eriksson, 1998). Post-Paleozoic tidal rhythmites include Jurassic (Kreisa and Moiola, 1986; Uhlir et al., 1988), Cretaceous (Allen, 1981; Ladipo, 1988; Rahmani, 1989; Eberth, 1996), Eocene (Yang and Nio, 1985; Santisteban and Taberner, 1988) and Miocene forms (Homewood and Allen, 1981; Allen and Homewood, 1984; Tessier and Gigot, 1989).

The other objective of the ancient tidal rhythmite research is to extract encoded palaeoastrophysical information (cf. Sonett et al., 1988; Kvale et al., 1999; Williams, 2000, 2004). It has been demonstrated that detailed mathematical-statistical analyses of the palaeotidal periodicities in combination with an understanding of tidal theory can be utilized to determine palaeolunar orbital dynamics and its temporal evolution (Rosenberg, 1997; Kvale et al., 1999; Williams, 2000, 2004). To unlock the palaeoastrophysical implications, it is therefore essential to determine reliable palaeolunar orbital periods from the ancient rhythmite record.

4.1. Palaeolunar orbital periods

To compute the ancient Earth–Moon distance (semimajor axis of the lunar orbit) and related palaeotidal and palaeorotational parameters, one must have a reasonable estimate of the palaeolunar sidereal orbital period (the time interval for the Moon to complete an orbit of the Earth when measured relative to the fixed stars). Kepler's third law states that the square of the orbital period of a planet is proportional to the cube of its mean distance from the sun. In the Earth–Moon system, this law can be mathematically expressed as follows:

$$(T_s/T_0)^2 = (a/a_0)^3 \tag{1}$$

where T_s and T_0 are the past and present lunar sidereal periods (length of the lunar sidereal month, present value is 27.32 solar days) and a and a_0 are the Earth–Moon distance (semimajor axis of the lunar orbit) in

the past and present (3.844×10^{10} cm), respectively. However, the lunar sideral orbital period cannot be determined directly from the rhythmite record since it is measured from a fixed point in the sky (cf. Runcorn, 1964, 1979a,b; Kvale et al., 1999; Eric P. Kvale, personal communication, 2003). It is, however, possible to determine the lunar synodic, tropical, and anomalistic periods directly from the rhythmite record. Thus, one has to depend solely on the relationship between the lunar synodic, tropical and sidereal orbital periods (Runcorn, 1964; Kvale et al., 1999, p. 1159–1160).

The conversion from tropical to sidereal period is straightforward because the periods are virtually the same (cf. Kvale et al., 1999). Thus, the tropical period can proxy for the sidereal period for all practical purpose. The present ratio of the lunar synodic (P_{syn}) to sidereal (P_{sid}) period is:

$$P_{syn}/P_{sid} = 29.5271/27.3186 = 1.0808 \qquad (2)$$

Kvale et al. (1999, p. 1159) proposed that this ratio can be safely used to convert from the synodic to the sidereal period over the last 1 billion years. Williams (2000), his Table 1 calculated the number of solar days per sidereal month (sideral period, t) during the Proterozoic from primary values derived from tidal rhythmites by applying following equation:

$$t = t_L/(1 + t_L/Y_D) \qquad (3)$$

where t_L and Y_D are number of solar days per synodic month and year (cf. Runcorn, 1964), respectively. A closer scrutiny of the palaeolunar orbital periods derived by Williams (2000), his Table 1, columns 2–5) from the 620, 900 and 2450 Ma old tidal rhythmites reveals that the ratio of the synodic to sidereal period ranges from 1.069 to 1.077. This, in turn, corroborates the suggestion of Kvale et al. (1999) that the variation of this ratio through geological time was very small (cf. Mazumder, 2002, 2004). The synodic to sidereal conversion ratio as evident from the 2450 Ma old Weeli Wolli Formation palaeotidal and palaeorotational data (Williams, 2000, his Table 1, column 3) is 1.07. By using a ratio of 1.07 as the synodic to sidereal period conversion factor, following the methodology proposed by Kvale et al. (1999, p. 1160–1161), the minimum number of solar days per sidereal month during the Chaibasa sedimentation

(late Paleoproterozoic) is determined to have been ~33.0/1.07=30.8. The only available quantitative Archaean tidal record is from the 3200 Ma old Moodies Group, South Africa (Eriksson and Simpson, 2000a,b). Mazumder (2001) estimated 26 lunar days in a synodic month during the Moodies sedimentation. However, Eriksson and Simpson (2001, p. 1160) argued that the Moodies spectral periods (23.6 and 13, Eriksson and Simpson, 2000a, their Fig. 5A,B) are a combination of semidiurnal and diurnal signatures and determination of lunar orbital periods (synodic and/or tropical) therefrom is difficult. However, Eriksson and Simpson (2000b) estimated a minimum of 18–20 days in a lunar sidereal orbital period at 3200 Ma. Subsequently, Eriksson and Simpson (2004) estimated that the minimum number of lunar days in a synodic month was 20 during the middle Archaean. Derivation of the lunar synodic and/or tropical periods during the Archaean is, thus, problematic. It must be mentioned that the relationship between the lunar synodic and sidereal period is related to the three-celestial body (Sun–Earth–Moon) problem, a longstanding question in astronomy and may be solved only by good quality tidal rhythmite data (Poppe L. de Boer, personal communication, 2003).

4.2. Calculating ancient Earth–Moon distance

To compute the ancient Earth–Moon distance, one has to start with Kepler's third law whose mathematical expression has been given in Eq. (1). The lunar sideral orbital period (length of the lunar sidereal month in terms of solar days) has a reciprocal relationship with the number of sidereal months (n) in a year (Kvale et al., 1999). From Kvale et al. (1999):

$$(n_0/n)^2 = (a/a_0)^3 \qquad (4)$$

where n and n_0 refer to the number of sidereal month per year in the past and present (13.37), respectively. Thus we must have some reasonable estimate of either T_s or n to compute the ancient Earth–Moon distance.

Effort has been made to compute the Earth–Moon distance for different geological period using palaeontological (Kahn and Pompea, 1978; Runcorn, 1979a,b and references therein), as well as, sedimentological (tidal rhythmite, Williams, 1989, 2000; Kvale et al., 1999) data. It must be noted that the

use of Kepler's third law of planetary motion alone to compute the semimajor axis of the lunar orbit (Earth–Moon distance) in the geological past is problematic (cf. Runcorn, 1979a,b). As in all physical processes, angular momentum and energy are conserved. While the Moon moves away from the Earth, its orbital angular momentum increases. On the other hand, the Earth's rotational angular momentum decreases: its rotation slows down and the length of day increases. In the geological past, the Moon was closer to the Earth and all its periods were therefore shorter. Although by the Kepler's third law of planetary motion the month was shorter in the past, assuming that lunar tidal friction has been causing the Moon to retreat from the Earth, the day length was proportionately even shorter: thus, the number of days in the month were greater and not smaller in the geological past (Runcorn, 1979a; Philip D. Nicholson, Cornell University, pers. commun., 2004). This is corroborated by the palaeotidal and palaeorotational parameters calculated from Precambrian tidal rhythmites (Williams, 2000, his Table 1). Kvale et al. (1999, p. 1166) calculated Pennsylvanian (~305 Ma) Earth–Moon distance from the Brazil tidal rhythmite data using both Eqs. (1) and (4) and the calculated distances are exactly same. The length of the sidereal month is usually expressed in terms of solar days/month whose present value is 27.32. The number of solar days in a Pennsylvanian (~305 Ma) lunar sidereal month was 27.27 (Kvale et al., 1999, their Fig. 12D), very close to its present value. Table 1 presents the calculated a/a_0 from the Precambrian palaeotidal data set given in Table 1 of Williams (2000) using Eqs. (1) and (4). As one goes further backward into the Precambrian, the number of days in

a month becomes greater and not smaller (Runcorn, 1979b; Williams, 2000, his Table 1). Therefore the a/a_0 ratio becomes greater than 1, which is geophysically impossible (see Kahn and Pompea, 1979 and references therein). Eriksson and Simpson (2000b) estimated the Earth–Moon distance of ca. 45–48 Earth radii at 3200 Ma using a lunar sidereal period of 18–20 days. These authors considered these are the minimum number of lunar days in a synodic month (see also Eriksson and Simpson, 2004). They have used the synodic to sidereal conversion factor of 1.0808 as proposed by Kvale et al. (1999) and calculated the then Earth–Moon distance (Ed. Simpson, personal communication, 2004).

Geologists calculate the length of sidereal month by dividing the length of the year by the number of sidereal months in a year (cf. Williams, 1989, 2000; Kvale et al., 1999). It is generally assumed that the length of the year is unchanged (cf. Kvale et al., 1999, p. 1161) or not significantly different from the present length of 31.56×10^6 s if there is no secular change in universal gravitational constant (G) (Williams, 2000, pp. 47 and 55). Recent experimental results have produced conflicting values of G (Gillies, 1997, his Tables 6 and 7) and, in spite of some progress and much interest, there remains to date no universally accepted way of predicting its absolute value. A related issue is the assignment of uncertainty to the absolute value of G. It has been argued that without a clear, confirmed relationship between G and any natural fundamental constant or measured physical quantity, very little else can be done on these issues (Gillies, 1997). Although Mars Viking Lander and lunar laser-ranging data indicate negligible change in planetary orbital radii implying thereby negligible planetary expansion (i.e.

Table 1
Calculated a/a_0 ratios from Precambrian tidal rhythmites (rhythmite data taken from Williams, 2000, his Table 1)

Age	2450 Ma Weeli Wolli	900 Ma[a] Big Cottonwood	900 Ma[b] Big Cottonwood	620 Ma Elatina	Modern
T_s	30.0	30.3	29.1	28.3	27.32 (T_0)
T_s/T_0	1.098	1.109	1.065	1.036	
$(a/a_0)T_s$	1.064	1.071	1.043	1.023	3.844×10^{10} cm (a_0)
n	15.5	15.3	14.5	14.1	13.37 (n_0)
n_0/n	0.862	0.874	0.922	0.948	
$(a/a_0)n$	0.906	0.914	0.947	0.965	

[a] Primary data after Sonett and Chan, 1998.
[b] Primary data after Sonett et al., 1996.

negligible change in G, Hellings et al., 1983; Chandler et al., 1993; Dickey et al., 1994; Williams, 2000), the possibility of secular change in G in the distant geological past, particularly during Precambrian cannot be ruled out (Creer, 1965; Glikson, 1980; Gillies, 1997). A secular decrease in the G value has been postulated by a number of researchers from theoretical and observational viewpoint (Branes and Dicke, 1961; Dicke, 1962; Runcorn, 1964, 1979b; Hoyle and Narlikar, 1972; Carey, 1975, 1976).

It has been argued that a postulated secular decrease in G (i.e. $Y<Y_0$) is not supported by morphologic studies of Mercury, Mars and the Moon as because these bodies show little or no evidence of expansion, an expected consequence of secular decrease in G value (cf. Crossley and Stevens, 1976; McElhinny et al., 1978; Williams, 2000, 2004). Also it has been claimed that calculation of possible changes in the Earth's radius, if there is any, from an examination of its surface features is not possible because of their continuous reshaping by a variety of geological processes since its origin (McElhinny et al., 1978). It must be noted that Crossley and Stevens (1976) have questioned but not ruled out the possibility of postulated secular decrease in G value. These authors clearly stated that the Mercury expansion might have taken place that has been entirely taken up in the unphotographed portions (Crossley and Stevens, 1976, p. 1724). Alternatively, some processes, such as thermal contraction during cooling, might have kept the volume nearly constant as G decreased (Crossley and Stevens, 1976). The enigma regarding the nature of unrecorded two-thirds to three-quarters of the Proterozoic crust on a globe of present-day dimensions can only be explained had the Earth's surface area grown with time (cf. Glikson, 1980).

4.3. Earth's moment of inertia

It has been claimed that the palaeotidal and palaeorotational data obtained from ancient tidal rhythmite can be used to test whether the Earth's moment of inertia, and thus the Earth's radius has been changed over geological time (cf. Runcorn, 1964; Williams, 2000, 2004). From Runcorn (1964)

$$1 - L/L_0 = (-1 + (I\omega Y_0 / I_0 \omega_0 Y)) / 4.83(1 + \beta) \tag{5}$$

where L/L_0 is the ratio of the past to the present lunar orbital angular momentum, I and I_0 are Earth's present and past moment of inertia, ω and ω_0 are Earth's present and past rotation rates, Y and Y_0 are lengths of the past and present years, β is the present ratio of solar to lunar retarding torques acting on Earth and 4.83 (Williams used a value 4.93 instead of 4.83 following Deubner, 1990, see Williams, 2000, pp. 54–55) is the present ratio of Moons orbital angular momentum to Earth's spin angular momentum and:

$$(L_0/L)^3 = T_0\omega / (Y_0 T_s) \tag{6}$$

Assuming no secular change in universal gravitational constant and, hence, putting $Y=Y_0$, Williams (2000) computed the I/I_0 ratio for different β values using the ~620 Ma old Elatina-Reynella palaeotidal and palaeorotational data set in Eqs. (5) and (6). He estimated the $I/I_0=1.006–1.014 (\pm 0.018)$ and claimed that the Elatina-Reynella rhythmite data argue against significant overall change in Earth's moment of inertia and thus Earth's expansion since ~620 Ma (Williams, 2000, p. 55; see also Williams, 2004). However, from Runcorn (1964, 1979a,b):

$$G^2 T_s / G_0^2 T_0 = (L/L_0)^3 \tag{7}$$

where G is not necessarily constant over geological time (Runcorn, 1979b, p. p1). Runcorn (1964, p. 824), considering the possibility that G varies inversely as the time since the origin of the Universe, calculated that $I>I_0$ (0.85 ± 0.003) for $\beta=1/3.7$ and $I>I_0$ (0.84 ± 0.003) for $\beta=1/5.5$. This implies that slow Earth expansion might have occurred if G varies (Runcorn, 1964, p. 825).

4.4. Internal self-consistency of palaeotidal and palaeorotational values

The accuracy of palaeotidal periods derived from the tidal rhythmites depends on the length as well as continuity of data (Williams, 1997, 2004). Measurement of successive bed/lamina thicknesses commonly provides an abbreviated palaeotidal period because of several reasons as discussed in Section 3.1. As a consequence, the spectra can have peaks shifted from true values (cf. Williams, 2000). It is therefore essential to recognize abbreviation in the raw data and consequent shifts of spectral periods for correct interpretation of the palaeotidal periods.

Williams (1991, 1997) proposed a methodology for testing the geophysical validity of the palaeotidal and palaeorotational parameters. He calculated the a/a_0 ratio by using independent primary values derived directly from the Neoproterozoic (~620 Ma) Elatina-Reynella rhythmite record using three different laws of celestial mechanics (cf. Williams, 2000, p. 50). Among these three equations, one (Kepler's third law of planetary motion) has already been discussed in the Sections 4.1 and 4.2. The other two laws are explained below.

The lunar nodal period (P, period of precession of the lunar orbit) depends on the Earth–Moon distance according to the following expression (after Kaula, 1969; Walker and Zahnle, 1986):

$$P = P_0[\cos i_0/\cos i](a_0/a)^{1.5} \qquad (8)$$

where the modern values are P_0=18.6 years, a_0= 3.84×10^{10} cm and i_0=5.15°, which is the inclination of the lunar orbit to the ecliptic. It is possible to calculate the Earth–Moon distance in the geological past if the ancient P and i values are known. The loss of the Earth's rotational angular momentum resulting from tidal friction of the Sun and the Moon and the change in lunar orbital angular momentum can be expressed as follows (Williams, 2000, p. 51):

$$1.219 - (1/4.93)(\omega/\omega_0)$$
$$= (a/a_0)^{1/2} + \left[(0.46)^2/13\right]\left[(a/a_0)^{13/2}\right] \qquad (9)$$

where ω_0 and ω are the Earth's present and past rotation rates, and the present ratio of the Moon's orbital angular momentum to the Earth's spin angular momentum=4.93 (after Deubner, 1990). It is thus possible to compute the (a/a_0) ratio if ω is known.

It has been suggested that if the calculated a/a_0 ratios using three different equations of celestial mechanics agree well, the palaeotidal and palaeorotational values are internally consistent and geophysically valid (Williams, 1989, 2000, 2004). Williams (2000) has demonstrated that ~620 Ma old Elatina-Reynella palaeotidal and palaeorotational values are internally self-consistent and geophysically valid. It is clear from Eqs. (1), (8), and (9) that one must determine T_s, P, i, and ω from the rhythmite record in order to compute the a/a_0 ratios. Among these four variables, i cannot be

determined from the rhythmite record (Williams assumed negligible change in i during the 0–620 Ma time span, but inclination of lunar orbit to the ecliptic in the distant geologic past, particularly during early Precambrian is solely a matter of speculation!). T_s and ω can be determined from the rhythmite data. The lunar nodal period, P, around ~900 Ma is unknown. Trendall (1973) suggested that the 23.3-year cyclicity preserved within the 2450 Ma old Weeli Wolli banded iron formation may represent a cycle equivalent to the modern double sunspot (Hale) cycle, but Walker and Zahnle (1986) reinterpreted it as an expression of the lunar nodal cycle (see also Trendall and Blockley, 2004). Subsequently, Williams (2000, his Table 1) derived P (21.6±0.7) from Weeli Wolli primary value using Eq. (8). It is therefore difficult to decide which value one should use in order to calculate the a/a_0 during the Paleoproterozoic. The lunar nodal period during 3200 Ma is also unknown. Therefore, the geophysical validity of the palaeotidal and palaeorotational values derived from the 900, 2450 and 3200 Ma old tidal rhythmites are unverified. As Williams (2004) pointed out, validated and internally self-consistent palaeotidal data that are in accordance with the laws of celestial mechanics are required to calculate reliable Earth's palaeorotational parameters.

5. Tidal rhythmite and palaeogeophysics: limitations

Analysis of ancient tidal rhythmite may help us to estimate the palaeolunar orbital periods in terms of lunar days/month accurately (cf. Williams, 1989, 2000; Archer, 1996a; Kvale et al., 1999; Kvale, 2003; Eriksson and Simpson, 2004). Determination of absolute Earth–Moon distances and Earth's palaeorotational parameters in the distant geological past from tidal rhythmite, however, is ambiguous because of the difficulties in determining the absolute length of the ancient lunar sidereal month (cf. Runcorn, 1979a,b; Kahn and Pompea, 1978, 1979). It is obvious that in the distant geological past, the Moon was closer to the Earth and all its orbital periods were therefore shorter. However, determination of the Earth–Moon distance in the distant geological past using Keplers third law of planetary motions require

absolute length of the sidereal month, not the number of days in a sidereal month. Recent experimental results have produced conflicting G values, and there remains today no universally accepted way of predicting the absolute value of G and also its uncertainty limit. Gillies (1997) clearly stated that

"In the absence of a bona fide theoretical prediction, and with the experimental results exhibiting the scatter that they do, the question becomes largely one of deciding on an algorithm for weighting (if appropriate) and averaging a set of existing measurements that satisfy suitable selection criteria."

The most intriguing and hitherto unsolved question about G is that of whether or not it is truly a constant at all, or if instead its value might be changing slowly with time (cf. Gillies, 1997). If so, the length of the year and Earth's moment of inertia was different in the geological past. The question is a fundamental one, and has been the focus of much thought over the last several decades. Without it, the calculated absolute Earth–Moon distances and Earth's palaeorotational parameters in the distant geologic past are highly speculative.

Acknowledgements

References

Adkins, R.M., Eriksson, K.A., 1998. Rhythmic sedimentation in a mid-Pennsylvanian delta front succession, Fourcorners Formation (Breathitt Group), eastern Kentucky: a near complete record of daily, semi-monthly tidal periodicities. In: Alexander, C.B., et al., (Eds.), Tidalites: Processes and Products, SEPM (Society for Sedimentary Geology) Special Publication, vol. 61, pp. 85–94.

Allen, J.R.L., 1981. Lower cretaceous tides revealed by cross-bedding with mud drapes. Nature 289, 579–581.

Allen, J.R.L., 1990. Salt-marsh growth and stratification: a numerical model with special reference to the Severn Estuary, southwest Britain. Marine Geology 95, 77–96.

Allen, P.A., Homewood, P., 1984. Evolution and mechanics of a Miocene tidal sandwave. Sedimentology 31, 63–81.

Archer, A.W., 1996a. Panthalassa: palaeotidal resonance and a global palaeoocean seiche. Palaeooceanography 11, 625–632.

Archer, A.W., 1996b. Reliability of lunar orbital periods extracted from ancient cyclic tidal rhythmites. Earth and Planetary Science Letters 141, 1–10.

Archer, A.W., Johnson, T.W., 1997. Modelling of cyclic tidal rhythmites (Carboniferous of Indiana and Kansas, Precambrian of Utah, USA) as a basis for reconstruction of intertidal positioning and palaeotidal regimes. Sedimentology 44, 991–1010.

Archer, A.W., Kvale, E.P., 1993. Origin of gray-shale lithofacies (clastic wedges) in U.S. midcontinental coal measures (Pennsylvanian): an alternative explanation. In: Cobb, J.C, Cecil, C.B (Eds.), Modern and ancient coal-forming environments. Geological Society of America Special Paper, vol. 286, pp. 181–192.

Archer, A.W., Kvale, E.P., Johnson, H.R., 1991. Analysis of modern equatorial tidal periodicies as a test of information encoded in ancient tidal rhythmites. In: Smith, D.G., Reinson, G.E., Zaitlin, B.A., Rahmani, R.A. (Eds.), Clastic Tidal Sedimentology. Memoir, vol. 16. Canadian Society of Petroleum Geologists, pp. 189–196.

Archer, A.W., Feldman, H.R., Kvale, E.P., Lanier, W.P., 1994. Comparison of drier- to wetter-interval estuarine roof facies in the Eastern and Western Interior Coal basins, USA. Palaeogeography, Palaeoclimatology, Palaeoecology 106, 171–185.

Archer, A.W., Kuecher, G.J., Kvale, E.P., 1995. The role of tidal-velocity asymmetries in the deposition of silty tidal rhythmites (Carboniferous, Eastern Interior Coal Basin U.S.A.). Journal of Sedimentary Research A65, 408–416.

Boothroyd, J.C., 1985. Tidal inlets and tidal deltas. In: Davis, R.A. (Ed.), Coastal Sedimentary Environments. Springer-Verlag, New York, pp. 445–532.

Bose, P.K., Mazumder, R., Sarkar, S., 1997. Tidal sandwaves and related storm deposits in the transgressive Protoproterozoic Chaibasa Formation, India. Precambrian Research 84, 63–81.

Branes, C., Dicke, R.H., 1961. Physical Review 124, 925.

Brown, J., Colling, A., Park, D., Phillips, J., Rothery, D., Wright, J., 1989. Waves, Tides and Shallow-Water Processes. Butterworth-Heinemann, 187 pp.

Brown, M.A., Archer, A.W., Kvale, E.P., 1990. Neap–spring tidal cyclicity in laminated carbonate channel-fill deposits and its implications Salem Limestone (Mississippian), south-central Utah. Geology 22, 791–794.

Carey, W.S., 1975. The expanding earth. Earth-Science Reviews 11, 105–143.

Carey, W.S., 1976. The Expanding Earth. Elsevier Science, New York, 488 pp.

Cattaneo, A., Steel, R.J., 2003. Transgressive deposits: a review of their variability. Earth Science Reviews 62, 187–228.

Chan, M.A., Kvale, E.P., Archer, A.W., Sonett, C.P., 1994. Oldest direct evidence of lunar–solar tidal forcing encoded in sedimentary rythmites, Proterozoic Big Cottonwood Formation, central Utah. Geology 22, 791–794.

Chandler, J.F., Reasenberg, R.D., Shapiro, I.I., 1993. New bound on *G*. Bulletin of the American Astronomical Society 25, 1233.

Creer, K.M., 1965. An expanding Earth? Nature 205, 539–544.

Crossley, D.J., Stevens, R.K., 1976. Expansion of the Earth due to a secular decrease in *G*—evidence from Mercury. Canadian Journal of Earth Sciences 13, 1723–1725.

Dalrymple, R.W, Makino, Y., 1989. Description and genesis of tidal bedding in the Cobequid Bay–Salmon river estuary, Bay of Fundy, Canada. In: Taira, A., Masuda, F. (Eds.), Sedimentary Facies of the active Plate Margin. Terra Publishing, Tokyo, pp. 151–177.

Dalrymple, R.W., Makino, Y., Zaitlin, B.A., 1991. Temporal and spatial patterns of Rhythmite deposition on mud flats in the macrotidal Cobequid Bayã Salmon river estuary, Bay of Fundy, Canada. Smith, D.G., Reinson, G.E., Zaitlin, B.A., Rahmani, R.A. Clastic Tidal Sedimentology, vol. 16. Canadian Society of Petroleum Geologists, Memoir, pp. 137–160.

de Boer, P.L., Oost, A.P., Visser, M.J., 1989. The diurnal inequality of the tide as a parameter for recognising tidal influences. Journal of Sedimentary Petrology 59, 912–921.

Deubner, F.L., 1990. Discussion on Late Precambrian tidal rhythmites in south Australia and the history of the Earth's rotation. Journal of the Geological Society (London) 147, 1083–1084.

Deynoux, M., Duringer, P., Khatib, R., Villeneuve, M., 1993. Laterally and vertically accreted tidal deposits in the upper Proterozoic Madina–Kouta Basin, southeastern Senegal, West Africa. Sedimentary Geology 84, 179–188.

Dicke, R.H., 1962. The Earth and cosmology. Science 138, 653–664.

Dickey, J.O., et al., 1994. Lunar laser ranging: a continuing legacy of the Apollo Program. Science 265, 482–490.

Eberth, D.A., 1996. Origin and significance of mud-filled incised valleys (Upper Cretaceous) in southern Alberta, Canada. Sedimentology 43, 459–477.

Eriksson, K.A., Simpson, E.L., 2000a. Quantifying the oldest tidal record: the 3.2 Ga Moodies Group, Barberton Greenstone Belt, South Africa. Geology 28, 831–834.

Eriksson, K.A., Simpson, E.L., 2000b. Archaean Earth–Moon dynamics deduced from tidalites in the 3.2 Ga Moodies Group, Barberton Greenstone belt, South Africa. Abstract no. BTH 59 GSA Annual Meeting, Reno, NV, p. A-307.

Eriksson, K.A., Simpson, E.L., 2001. Quantifying the oldest tidal record: the 3.2 Ga Moodies Group Barberton Greenstone Belt, South Africa: Reply. Geology 29, 1159–1160.

Eriksson, K.A., Simpson, E.L., 2004. Precambrian tidalites: recognition and significance. In: Eriksson, P.G., Altermann, W., Nelson, D., Mueller, W., Cateneau, O., Strand, K. (Eds.), Tempos and Events in Precambrian Time. Developments in Precambrian Geology 12. Elsevier, Amsterdam, pp. 631–642.

Eriksson, P.G., Condie, K.C., Trisgaard, H., Muller, W., Altermann, W., Catunean, O., Chiarenzali, J., 1998. Precambrian clastic sedimentation systems. Sedimentary Geology 120, 5–53.

Fairbridge, R.W., Sanders, J.E., 1987. The Sun's orbit, A.D. 750–2050: basis for new perspectives on planetary dynamics and Earth–Moon linkage. In: Rampino, M.R., Sanders, J.E., Newman, W.S., Königsson, L.K. (Eds.), Climate, History, Periodicity, and Predictability. Nostrand Reinhold, New York, pp. 446–471.

FritzGerald, D.M., Nummedal, D., 1983. Response characteristics of an ebb-dominated tidal inlet channel. Journal of Sedimentary Petrology 53, 833–845.

Ghosh, S.K., Chakraborty, C., Chakraborty, C., 2004. Combined tide and wave influence on sedimentation of Lower Gondwana coal measures of central India: Barakar Formation (Permian), Satpura basin. Journal of the Geological Society (London) 161, 117–131.

Gillies, G.T., 1997. The Newtonian gravitational constant: recent measurements and related studies. Reports on Progress in Physics 60, 151–225.

Glikson, A.Y., 1980. Precambrian sial–sima relations: evidence for Earth expansion. Tectonophysics 63, 193–234.

Greb, S.F., Archer, A.W., 1995. Rhythmic sedimentation in a mixed tide and wave Deposit, Hazel Patch Sandstone (Pennsylvanian), eastern Kentucky coal Field. Journal of Sedimentary Research B65, 93–106.

Hellings, R.W., Adams, P.J., Anderson, J.D., Keesey, M.S., Lau, E.L., Standish, E.M., Canuto, V.M., Goldman, I., 1983. Experimental test of the variability of *G* using Viking Lander ranging data. Physical Review Letters 51, 1609–1612.

Homewood, P., Allen, P.A., 1981. Wave-, tide-, and current controlled sandbodies of Miocene Molasse, western Switzerland. American Association of Petroleum Geologists Bulletin 65, 2534–2545.

Horne, J.H., Baliunas, S.L., 1986. A prescription for period analysis of unevenly sampled time series. Astrophysical Journal 302, 757–763.

Hoyle, F., Narlikar, J.V., 1972. Cosmological models in a conformally invariant gravitational theory—II. Monthly Notices of the Royal Astronomical Society 155, 323–335.

Jenkins, G.M., Watts, D.G., 1968. Spectral analysis and its applications. Holden-Day, New York.

Kahn, P.G.K., Pompea, S.M., 1978. Nautiloid growth rhythms and dynamical evolution of the Earth–Moon system. Nature 275, 606–611.

Kahn, P.G.K., Pompea, S.M., 1979. Nautiloid growth rhythms and lunar dynamics—reply to comments by S.K. Runcorn. Nature 279, 453.

Kaula, W.M., 1969. An Introduction to Planetary Physics. Wiley, Toronto.

Kaye, C.A., Stuckey, G.W., 1973. Nodal tidal cycle of 18.6 yr: its importance in sea-level curves of the east coast of the United

States and its value in explaining long-term sea-level changes. Geology 1, 141–144.

Kreisa, R.D., Moiola, R.J., 1986. Sigmoidal tidal bundles and other tide-generated sedimentary structures of the Curtis Formation Utah. Geological Society of America Bulletin 97, 381–387.

Kuecher, G.J., Woodland, B.G., Broadhurst, F.M., 1990. Evidence of deposition from individual tides and of tidal cycles from the Francis Creek Shale (host Rock to the Mazon Creek Biota), Westphalian D (Pennsylvanian), northeastern Illinois. Sedimentary Geology 68, 211–221.

Kvale, E.P., 2003. Tides and tidal rhythmites. In: Middleton, G.V. (Ed.), Encyclopedia of Sediments and Sedimentary Rocks. Kluwer Academic.

Kvale, E.P., Archer, A.W., Johnson, H.R., 1989. Daily, monthly, and yearly tidal cycles within laminated siltstones of the Mansfield Formation (Pennsylvanian) of Indiana. Geology 17, 365–368.

Kvale, E.P., Fraser, G.S., Archer, A.W., Zawistoski, A., Kemp, N., McGough, P., 1994. Evidence of seasonal precipitation in Pennsylvanian sediments of the Illinois Basin. Geology 22, 331–334.

Kvale, E.P., Cutright, J., Bilodeau, D., Archer, A.W., Johnson, H.R., Pickett, B., 1995. Analysis of modern tides and implications for ancient tidalites. Continental Shelf Research 15, 1921–1943.

Kvale, E.P., Johnson, H.W., Sonett, C.P., Archer, A.W., Zawistoski, A., 1999. Calculating lunar retreat rates using tidal rhythmites. Journal of Sedimentary Research 69, 1154–1168.

Ladipo, K.O., 1988. Example of tidal current periodicity from an Upper Cretaceous sandstone succession (Anambra basin, SE. Nigeria). In: de Boer, P.L, et al., (Eds.), Tide Influenced Sedimentary Environment and Facies. D. Reidel, Dordrecht, pp. 333–340.

Lisitzin, E., 1974. Sea level changes. Elsevier Oceanography Series, 8. Elsevier, Amsterdam. 286 pp.

Macmillan, D.H., 1966. Tides. American Elsevier, New York, 240 pp.

Marchuk, G.I., Kagan, B.A., 1989. Dynamics of Ocean Tides. Kluwer, Dordrecht, 327 pp.

Martino, R.L., Sanderson, D.D., 1993. Fourier and autocorrelation analysis of Estuarine tidal rhythmites, Lower Breathitt Formation (Pennsylvanian), eastern Kentucky, USA. Journal of Sedimentary Petrology 63, 105–119.

Mazumder, R., 2001. Quantifying the oldest tidal record: the 3.2 Ga Moodies Group, Barberton Greenstone Belt, South Africa—comment. Geology 29, 1159–1160.

Mazumder, R, 2002. Sedimentation history of the Dhanjori and Chaibasa formations, eastern India and its implications. Unpublished PhD dissertation, Department of Geological Sciences Jadavpur University, Kolkata, 119 pp.

Mazumder, R., 2004. Implications of lunar orbital periodicity from the Chaibasa tidal rhythmite (India) of late Paleoproterozoic age. Geology, in press.

Mazumder, R., Bose, P.K., Sarkar, S., 2000. A commentary on the tectono-sedimentary record of the pre-2.0Ga. Continental growth of India vis. a vis. a pre-Gondwana Afro-Indian supercontinent. J. African Earth Sci. 30, 201–217.

McElhinny, M.W., Taylor, S.R., Stevenson, D.J., 1978. Limits to the expansion of Earth, Moon Mars and Mercury and to changes in the gravitational constant. Nature 271, 316–321.

Miller, D., Eriksson, K.A., 1997. Late Mississippian Prodeltaic rhythmites in the Appalachian basin: a hierarchical record of tidal and climatic periodicities. Journal of Sedimentary Research 67, 653–660.

Mueller, W.U., Corcoran, P.L., Donaldson, J.A., 2002. Sedimentology of tide- and wave-influenced high-energy Archaean coastline: the Jackson Lake Formation, Slave province, Canada. In: Altermann, W., Corcoran, P. (Eds.), Special Publication International Association of Sedimentologists, vol. 33, pp. 153–182.

Naha, K., 1965. Metamorphism in relation to stratigraphy, structure and movements in parts of east Singhbhum, Eastern India. Quaternary Journal of Geological Mining, Mineralogical and Metallurgical Society of India 37, 41–88.

Oost, A.P., de Haas, H., Ijensen, F., van den Boogert, J.M., de Boer, P.L., 1993. The 18.6 yr nodal cycle and its impact on tidal sedimentation. Sedimentary Geology 87, 1–11.

Piper, J.D.A., 1990. Implications of some recent sedimentological studies to the history of the Earth–Moon system. In: Brosche, P., Sündermann, J. (Eds.), Earth's rotation from Eons to Days. New York, Springer-Verlag, pp. 227–233.

Press, W.H., Flannery, B.P., Teukolsky, S.A., Vetterling, W.T., 1989. Numerical recipes: the Art of Scientific computing. Cambridge University Press, Cambridge, UK, 702 pp.

Pugh, D.T., 1987. Tides, Surges and Mean Sea Level. Wiley, New York, 472 pp.

Rahmani, R.A., 1989. Cretaceous tidal estuarine and deltaic deposits, Drumheller, Alberta, Field Trip Guidebook. Second International Research Symposium on Clastic Tidal deposits, Calgary, Alberta, Canada.

Rosenberg, G.D., 1997. How long was the day of the Dinosaur? And why does it matter? In: Wolberg, D.L., Stump, E., Rosenberg, G.D. (Eds.), Dinofest International, Proceedings of a Symposium Sponsored by Arizona State University. The Academy of Sciences, Philadelphia, pp. 493–512.

Runcorn, S.K., 1964. Changes in the Earth's moment of inertia. Nature 204, 823–825.

Runcorn, S.K., 1979a. Nautiloid growth rhythms and lunar dynamics—comment. Nature 279, 452–453.

Runcorn, S.K., 1979b. Palaeontological data on the history of the Earth–Moon System. Physics of the Earth and Planetary Science Interior 20, 1–5.

Russell, R.C.H., MacMillan, D.H., 1970. Waves and tides. Greenwood Press, Westport, CN, 348 pp.

Saha, A.K., 1994. Crustal evolution of Singhbhum-North Orissa, Eastern India. Memoir-Geological Society of India 27, 341 pp.

Santisteban, C., Taberner, C., 1988. Geometry, structure and geodynamics of a sandwave complex in the southeast margin of the Eocene Catalan Basin, Spain. In: de Boer, P.L, et al., (Eds.), Tide Influenced Sedimentary Environment and Facies. D. Reidel, Dordrecht, pp. 123–138.

Sonett, C.P., Chan, M.A., 1998. Neoproterozoic Earth–Moon dynamics: rework of the 900 Ma Big Cottonwood Canyon tidal laminae. Geophysical Research Letters 25, 539–542.

Sonett, C.P., Finney, S.A., Williams, C.R., 1988. The lunar orbit in the late Precambrian and the Elatina sandstone laminae. Nature 335, 806–808.

Sonett, C.P., Kvale, E.P., Zakharian, A., Chan, M.A., Demko, T.M., 1996. Late Proterozoic and Paleozoic tides, retreat of the Moon, and rotation of the earth. Science 273, 100–104.

Stowe, K., 1987. Essentials of Ocean Science. Wiley, New York. 353 pp.

Tape, C.H., Cowan, C.A., Runkel, A.C., 2003. Tidal bundle sequences in the Jordan Sandstone (Upper Cambrian), southeastern Minnesota, U.S.A.: evidence for tides along inboard shorelines of the Sauk epicontinental sea. Journal of Sedimentary Research 73, 354–366.

Tessier, B., Gigot, P., 1989. A vertical record of different tidal cyclicities: an example from the Miocene marine molasses of Digne (Haute Provenance France). Sedimentology 36, 767–776.

Tessier, B., Archer, A.W., Lanier, W.P., Feldman, H.R., 1995. Comparison of Ancient tidal rhythmites (Carboniferous of Kansas and Indiana, USA) with Modern analogues (the Bay of Mont-Saint-Michel, France). Special Publication of the International Association of Sedimentologists 24, 259–271.

Trendall, A.F., Blockley, J.G., 2004. Precambrian iron-formation. In: Eriksson, P.G., Altermann, W., Nelson, D., Mueller, W., Catuneau, O., Strand, K. (Eds.), Tempos and Events in Precambrian Time: Developments in Precambrian Geology 12. Elsevier Science, Amsterdam, pp. 403–421.

Trendall, A.F., 1973. Varve cycles in the Weeli Wolli Formation of the Precambrian Hamersley Group, Western Australia. Economic Geology 68, 1089–1097.

Trisgaard, H., 1993. The architecture of Precambrian high energy tidal channel deposits: an example from the Lyell Lond Group (Eloomore Bay Supergroup), northeast Greenland. Sedimentary Geology 88, 137–152.

Uhlir, D.M., Akers, A., Vondra, C.F., 1988. Tidal inlet sequence, Sundane Formation (Upper Jurassic), North-central Wyoming. Sedimentology 35, 739–752.

Walker, J.C.G., Zahnle, K.J., 1986. Lunar nodal tide and distance to the Moon during the Precambrian. Nature 320, 600–602.

Wells, J.T., Coleman, J.M., 1981. Periodic mudflat progradation, northeastern coast of South America: a hypothesis. Journal of Sedimentary Petrology 51, 1069–1075.

Williams, G.E., 1989. Late Proterozoic tidal rhythmites in South Australia and the history of the earth rotation. Journal of the Geological Society (London) 146, 97–111.

Williams, G.E., 1991. Upper Proterozoic tidal rhythmites, South Australia: sedimentary features, deposition, and implications for the earth's palaeorotation. In: Smith, D.G., Reinson, G.E., Zaitlin, B.A., Rahmani, R.A. (Eds.), Clastic Tidal Sedimentology, Canadian Society of Petroleum Geologists, Memoir, vol. 16, pp. 161–177.

Williams, G.E., 1997. Precambrian length of day and the validity of tidal rhythmite paleotidal values. Geophysical Research Letters 24, 421–424.

Williams, G.E., 2000. Geological constraints on the Precambrian history of Earth's rotation and the Moon's orbit. Reviews of Geophysics 38, 37–59.

Williams, G.E., 2004. Earth's Precambrian rotation and the evolving lunar orbit: implications of tidal rhythmite data for palae-ogeophysics. In: Eriksson, P.G., Altermann, W., Nelson, D., Mueller, W., Cateneau, O., Strand, K. (Eds.), The Precambrian Earth—Tempos and Events Developments in Precambrian Geology, vol. 12. Elsevier, Amsterdam, pp. 473–482.

Yang, C.S., Nio, S.D., 1985. The estimation of paleohydrodynamic processes from subtidal deposits using time series analysis methods. Sedimentology 32, 41–57.

Zaitlin, B.A., 1987. Sedimentology of the Cobeuid Bay–Salmon river estuary, Bay of Fundy, Canada, Unpublished PhD thesis, Queen's University, Kingston, Ontario, 391 pp.

Rajat Mazumder is a sedimentologist. Graduating from Durgapur Government College, Burdwan University in 1989, he did his Postgraduate from Allahabad University in 1991. He did his PhD from Jadavpur University, Kolkata on sedimentation history of two Paleoproterozoic siliciclastic formations of eastern India in 2002. Mazumder is a Senior Lecturer in Geology, Asutosh College, Kolkata and at present he is working as a JSPS Post Doctoral Fellow at Yokohama National University, Japan. His present interest is in volcano-sedimentary successions developed on the Archaean and Paleoproterozoic cratons. Presently, he is on study leave from Asutosh College and working on the late Paleoproterozoic supracrustals of the Singhbhum crustal province, India in collaboration with Prof. M. Arima. Reconstruction of sedimentary sequence-building processes in the context of palaeogeographic shifts under overriding control of Tectonism and sea level change is his passion. He has been recently awarded Alexander von Humboldt Post Doctoral fellowship to work with Prof. W. Altermann at Munich University, Germany. Mazumder believes that deduction is science not speculation but logical speculation is a must for deduction.

Makoto Arima is an Experimental Petrologist. He completed his Postgraduate and DSc dissertation from Department of Geology and Mineralogy, Hokkaido University, Japan in 1974 and 1977, respectively. He then spent about a year as JSPS Post Doctoral Fellow at Hokkaido University. Subsequently, he worked as a Research Associate with Prof. A. Edgar at Department of Geology, University of Western Ontario, Canada. He joined Yokohama National University as an Associate Professor in 1986. At present, he is a Professor of Geology at Graduate School of Environment and Information Sciences, Yokohama National University. Arima's current research interest includes Upper mantle and lower crustal processes, continental crustal growth and evolution of intra-oceanic arc systems. Geology is his first love and he believes in multidisciplinary research to solve geological and environmental problems.